APPLIED
MATERIALS
AND TECHNOLOGY

Research Article

Jamt.ejournal.unri.ac.id

The Flue Gas Desulfurization Gypsum Applications in Production of Eco-Friendly Cementitious Matrices

R. H. N. Bibiano, Juliana de C. Izidoro, Denise A. Fungaro *

Centre Instituto de Pesquisas Energéticas e Nucleares, IPEN-CNEN/SP, São Paulo, SP, Brazil

ABSTRACT: Portland cement is one of the most manufactured materials in the world. The worldwide cement industry accounts for at least 5-8% of the anthropogenic CO_2 emissions and, therefore is an important sector for CO_2-emission mitigation strategies to limit global warming. One of the strategies for reducing the carbon footprint of the cement industry is to replace traditional Portland cement with other solid wastes. In the present study, the influence of the application of flue gas desulfurization gypsum (FGD gypsum) generated from coal-fired power plant in construction mortar was investigated. Cylindrical specimens were molded with Portland cement type CPII-F 32, sand and 0%, 25%, 50% and 75% amounts of FGD gypsum. After curing time of 1, 3, 7, 28 and 91 days, the cementitious materials were characterized mechanically by axial compressive strength, setting time and slump. The pastes in the age of 28 days were further characterized by X-ray diffraction with Rietveld analysis.Results showed that FGD gypsum can be used as a substitute for cement as a setting retarder in an amount of up to 25%, and as an accelerator in an amount of 75%, being necessary dosage of the specific traces of the materials depending on the purpose of its use.

Key words: FGD gypsum, characterization, recycling, cement

1. INTRODUCTION

Sustainability in construction requires the reduction of the consumption of natural resources, especially energy, water and materials. Regarding the emission of gases, the cement production is responsible for about 5–8% of the global CO_2 emissions (2.8 Gtons/y). [1-3]. CO_2 is a major contributor for the greenhouse effect and therefore responsible for global warming of the planet [4].

Reducing greenhouse gas emissions is one of the major reasons for replacing Portland cement by alternative materials contributing to reduced use of cementitious clinker [5-7].

Flue gas desulfurization (FGD) is the most used technology for remove up to 99% of the sulfur oxides in flue gases for a typical conventional coal-fired power plant. The process involves the removal of SO_2 from flue gas using an alkaline sorbent, usually limestone. The wet method produces FGD by-product (FGD gypsum) composed predominantly of sulfate dihydrate [8, 9].

Large volumes of FGD gypsum are continuously produced and generally remain in landfills on the surrounding of the coal-fired thermal plant resulting in possible contamination of soil and groundwater. Thus, the potential use as a cement replacement can significantly reduce the environmental impact.

Previous studies have shown that FGD gypsum can be used as alternative in various materials employed in the construction industry [10-13]. The characteristics of FGD gypsum samples varies according to the proportion of limestone used for the desulfurization process and the type of coal used. The aim of this study was to evaluate the use of FGD gypsum generated in a coal-fired thermoelectric plant as a partial replacement for Portland cement in the production of cementitious matrices.

2. MATERIAL AND METHODS

2.1 Material

All chemicals used were of analytical grade. The waste produced from the wet flue gas desulfurization process (FGD gypsum) was collected at Pampa Sul Thermoelectric Power Plant, located in the Candiota, RS, Brazil. For the composition of the mortar were used commercial Portland cement type CPII-F 32 according to Brazilian Standard [14] and the Brazilian standard sand [15] provided by IPT (Institute for Technological Research, SP, São Paulo, Brazil).

2.2 Methods

The chemical composition of CPII-F 32 and FGD was evaluated by X-ray fluorescence (XRF) using a Panalytical Minipal Cement16, from molten pellets in a Claisse model M4 melting machine, fluxes based on a mixture of lithium tetraborate/lithium metaborate of the MAXXIFLUX brand (66.67% $Li_2B_4O_7$, 32.83% $LiBO_2$ and 0 .7% LiBr), with a

Received : September 16, 2023
Revised : October 25, 2023
Accepted : November 13, 2023

with a proportion of 1.0 g of sample and 6.75 g of flux. The mineralogical composition of materials was determined by X -ray diffraction (Rigaku – Multiflex) using Cu Kα radiation at 40 kV and 20 mA. The Match3 Rietveld FullProf software was employed to analyse the obtained diffractograms.

2.2.1 Material characterization

Materials were characterized in accordance with the Brazilian standards ABNT NBR. The tests were performed in triplicate and respecting the maximum difference of results, as defined in the applicable standards. The following laboratory tests were carried out for: (a) Portland cement CPII-F 32 and FGD: Loss on ignition [16]; XFR [17]; Free CaO [18]; Insoluble residue [19]; CO_2 [20]; Fineness [21]; Specific mass [22]; XDR [17, 23]; SO_2 and SO_3 [20]; Moisture Content [24]; Setting time [25]; Specific surface area [26]; Water content [27]; Pozzolanic activity [28]; Pozzolanic activity index [29]; (b) Sand: Granulometric analysis [15, 30, 31]; Fineness modulus classification [15, 30, 32]; Specific mass [33].

2.2.2 Cement matrices characterization

Cylindrical specimens were molded with Portland cement CPII-F 32, sand and 0%, 25%, 50% and 75% amounts of FGD gypsum. The number of replicates depends on each test specified in the Standards. The mixture without FGD used as reference was labelled as FGD0. The other mixtures were labelled as FGD25, FGD50 and FGD75 for 25%, 50% and 75% of FGD as cement substitute, respectively. The fresh-state tests were carried out accordance with Brazilian Standards (ABNT/NBR): normal paste consistency [27]; mixture and molding of cylindrical specimens with a diameter of 50 mm × height of 100 mm [34], setting time [25]; preparation and adaptation of the control and curing chambers [35]. The amount of water necessary to obtain the normal consistency of the cement paste was calculated according to previous study [36].

In the hardened state, axial compressive strength was tested at different ages (3, 7, 28 and 90 days after molding), according to Brazilian Standards (ABNT NBR): [34, 37]. Others tests performed were: Slump tests [38]; XDR [17, 23]. An environmental characterization of the cement matrices was carried out through leaching tests [39] and solubilization [40]. The material were classified as "hazardous" (class I) or "non-hazardous" (II-A non-inert, and II-B inert) according to the Brazilian standard [41].

3. RESULT AND DISCUSSION

3.1 Characterization of cement CP II-F 32

The chemical composition and properties of the cement CPII-F 32 are summarized in Table 1. According to Table 1, the chemical composition indicates a predominance of calcium oxide and silicon dioxide, as expected for this type of cement [42].

Characteristics of Portland cement are primarily influenced by the relative amounts of metal oxides present in the clinker. An approximate composition of the main oxides present in typical cement clinker is: CaO 60-67%, SiO_2 17-25 %, Al_2O_3 3-8%, Fe_2O_3 0.5-6%, MgO 0.1-4 and SO_3 0.7-3 [11, 13, 43, 44].

Sulfuric Anhydride (SO_3) content in the cement must remain equal to or below 4.5% by mass, otherwise secondary reactions may occur after cement hydration forming by-products that can contribute to the reduction of its strength [45, 46]. As can be seen in Table1, the sulfuric anhydride content is within parameters established by the standard.

The loss on ignition (LOI) content indicates the hydration and carbonation limit of the free oxides, mainly calcium, magnesium and potassium oxides, due to the exposure of the cement to the air. The higher the LOI content, the greater the amount of carbon present in the material. For cement CPII-F 32, the limit content must be equal to or less than 12.5% by mass [45]. The cement presented a LOI value within the parameters established by the standard.

Table 1 Chemical composition and properties of the cement CPII-F 32

Properties	Result
CaO (wt%)	55.30
SiO_2 (wt%)	18.10
MgO (wt%)	4.89
Al_2O_3 (wt%)	4,32
SO_3 (wt%)	3.44
Fe_2O_3 (wt%)	2.87
K_2O (wt%)	0.88
TiO_2 (wt%)	0.19
P_2O_5 (wt%)	0.14
Mn_2O_3 (wt%)	0.14
ZnO (wt%)	0.06
SrO (wt%)	0.06
Cr_2O_3 (wt%)	0.01
Free CaO (%)	1.39
Insoluble residue (%)	5.07
CO_2 (%)	7.55
Loss on ignition (%)	9.56

Regarding the insoluble residue (IR) present in the cement sample, the partial insolubility of the clinker is taken into account, that is, the non-reactive portion of the material, which must have a limit parameter of 7.5% by mass for cement CPII-F 32 [45]. The IR is within the parameters established by the standard.

Table 2 shows the fineness modules, specific surface area, amount of water require for normal consistency of cement paste, setting time and the main mechanical strengths of cement CPII F-32. These properties establish the quality parameters of the cement.

The initial of setting time is the total time from the contact of the cement with water until the beginning of the paste hardening phase, while the final of setting time is the total time since the contact of the cement with water until the end of the paste hardening phase. The fineness modules and specific surface area indicate the level of hydration of cement grains when in contact with water. The percentage of water to obtain a paste of normal consistency implies the ideal amount of water for total hydration of pastes composed of cement and water, so that their workability is permissible, i.e. handling and moldability. The specific mass is within the range observed for Brazilian cements (2.98 to 3.12 g/cm^3). The mechanical resistance to axial compression at 3, 7 and 28 days are parameters that indicated the evolution of hydration of the mortar composed of cement, sand and water, consequently controlling the increase in mortar resistance.

Table 2. Physical and mechanical properties of CPII-F 32

Properties		Result
Setting Time	Initial (min)	318.2
	Final (min)	370.5
Specific surface area (cm^2/g)		4358
Water content (%)		25.94
Specific mass (g/cm^3)		3.02
Fineness	# 200	1.73
	# 325	8.32
Compressive strength (Mpa)	3 days	23.79
	7 days	28.32
	28 days	33.56

The X-ray diffraction of Portland cement was performed to identify the compounds of crystalline phases. As presented in Fig. 1, the Rietveld analysis identified and quantified the following phases: 27.7% of C_2S, 44.6% of C_3S, 5.70% of C_3A, 11.1% of C_4AF and 10.9% of CS. Tricalcium silicate (C_3S) and dicalcium silicate (C_2S) are the most important compounds responsible for strength, representing 72.3% of the material. In addition to the major phases, CPII-F 32 also contain so-called minor components (C_4AF, CS and C_3A), whose formation strongly depends on the minor elements present in the raw mixture for clinker. The crystalline phases contents are within the range reported in previous studies [43, 44, 47, 48].

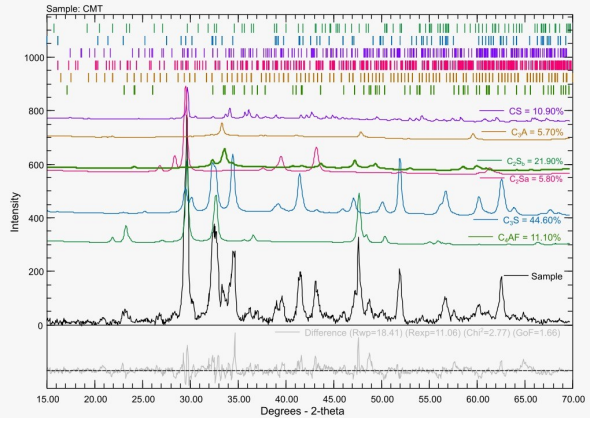

Fig. 1. X-ray diffractogram of the cement CPII-F 32

3.2 Characterization of FGD

The composition and percentage of FGD gypsum may vary depending on their origin. The chemical composition of FGD waste and loss on ignition obtained by X-ray fluorescence is given in Table. 3. The major constituents were S, Ca, Si, and Al and others elements were present with concentrations below 1.0 wt %. The percentage of elements is within the range usually encountered in FDG gypsum, suggesting its use as construction material [10, 11].

The high amount of CaO could be beneficial because it can contribute to the pozzolanic reaction by improving the performance at later ages [49]. On the other hand, the SO_3 content could affect the setting time of speciments containing amounts of FGD depending on the dosage [50].

FGD gypsum presented fineness index higher compared to cement. In previous studies, FGD gypsum specific mass values were between 2.19 to 3.13 g/cm^3. This difference was attributed to the type of coal and the combustion process used to burn it [48, 51-54].

Table 4 show the results for the evaluation of pozzolanic activity regarding the physical properties of FGD sample. The pozzolanic activity index showed that greater the FGD addition in the replacement of the cement, lower the performance in the mechanical strength of axial compression.

In the analysis by X-ray diffraction of the FGD (Fig. 2), the phases found from the refinement by the Rietveld method were 7.38% of calcium silicate ($CaSiO_3$), 0.53% of manganese silicate or braunite (Mn_6SiO_{12}), 1.99% of silica (SiO_2) and 1.05% of calcium carbonate ($CaCO_3$). It was observed, predominantly, the amounts of 46.9% and 42.2% of the phases of calcium sulfate hemihydrate ($CaSO_4.1/2H_2O$) and calcium sulfate dihydrate ($CaSO_4.2H_2O$), respectively. The $CaSO_4$ content present in FGD gypsum samples generated in ten thermoelectric power plants varied from 51.8–89% [55].

Table 3. Physico-chemical properties of FGD sample

Properties	Result
SO_3 (wt%)	47.9
CaO (wt%)	26.3
SiO_2 (wt%)	2.50
Al_2O_3 (wt%)	1.00
Fe_2O_3 (wt%)	0.40
P_2O_5 (wt%)	0.40
K_2O (wt%)	0.20
MgO (wt%)	0.10
ZnO (wt%)	0.10
TiO_2 (wt%)	0.10
Others oxides (wt%)	< 0.10
Insoluble residue (%)	4.50
CO_2 (%)	1.19
Loss on ignition (%)	21.0
Fineness (%)	12.303
Specific mass (g/cm³)	2.45

Table 4. Pozzolanic activity of FGD in terms of physical properties

Test		Result
Pozzolanic activity with lime at 7 days (Mpa)		3.4
Pozzolanic activity index with cement (Mpa)	FGD (%)	Resistance
	0	37.1
	25	10.9
	50	6.02
	75	3.01

3.3 Characterization Tests of Fine Aggregate

The results obtained in the characterization tests of fine aggregate are presented in Table 5. It is possible to verify that the studied aggregate is a sand formed by medium size grains [11].

3.4 Characterization of Cement Matrices

3.4.1 Characterization of fresh state

The results of the mortar fresh state tests are shown in Table 6. The greater demand for water that would allow the workability of the mortar brought a consequent increase in

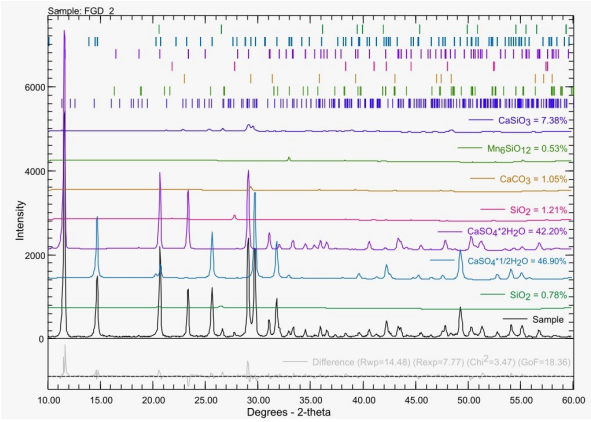

Fig. 2. X-ray diffractogram of FGD

the hydration time of the pastes with 25% and 50% of FGD. For the pastes with 75% of FGD, there were a notable increase in the initial and final setting time, as well as in the consistency test. This cement paste went into the hardened state after 3 min of contacting with water and after 5 min the needle of the device no longer penetrated the paste. Thus, the properties of the matrix were highly affected due to the inclusion of the high content of FGD.

The setting times for FGD25 and FGD 50 specimens were not determined due to not presenting the initial setting time for the hardened state after more than 350 min.

3.4.2 Characterization of hardened state

The moldings of the specimens were carried out with cylindrical shapes of 50 mm in diameter by 100 mm in height. The materials consumption for the concrete mixes design is presented in Table 7. All specimens were demolded after 24 h after production of concrete and were put in a curing tank before rupture.

The specimens were ruptured by axial compression at the ages of 1, 3, 7, 28 and 91 days and the results can be observed in the Table 8. The reference specimens (FGD0) showed values similar to those presented in the Table 2. It was also possible to observe that there was a decrease in strength for all samples with replacement, which could not be discarded, that there was also an extension in the hydration time, which delayed the setting times of mortars of all ages.

Table 5. Physico-chemical properties of FGD sample

Properties	Results
Moisture (%)	8.2
Specific mass (g/cm³)	2.59
Fineness modulus	2.06
Maximum size (mm)	2.4

The extension of the hydration time caused the hydration of the cement grains occur more homogeneously and, as a consequence, the resistance deviations between each specimens with FGD replacement were much smaller, or almost zero, compared to the reference specimen. It is possible to observe the "hourglass" shape in the rupture of the specimens, indicating that FGD has satisfactory hydration properties in cement (Fig. 3).

The molding of the specimens with 75% replacement was only possible with the correction of the water/cement ratio to a value above the limits of the standard, thus guaranteeing the abatement of the pastes and consequently increasing the useful time in the molding process in the form. At this percentage of replacement, a rapid hardening of the pastes occurs, and therefore, the specimens were molded only for the age of 28 days, in order to obtain the measurement of the performance index with the pozzolanic material. Results from slump test showed that the consistency of specimens with residue decreased (~ 5%) in relation to the mixture without FGD used as reference (FGD0), however, there was no variation in the value with the increase in the amount of FGD.

The XRD analyses of the cement paste (CP) at 1, 3, 7, 28 and 91 days with different FGD contents are shown in Fig. 4. As shown in Fig. 4a, was observed the increase in crystallinity in the formation of hydrated calcium silicate (CSH) and calcium aluminium sulfate hydroxide (AFt -ettringite) phases, which is defined in greater quantity after 7 days of hydration, and the fixation of portlandite (CH). A reduction in alite (C_3S) and celite (C_3A) peaks responsible for the initial reactions of cement in the first ages was also observed. As the curing time increased, increased the peaks corresponding to the formation of sulfates ettringite (CS'H) and portlandite (CH) resulting from the dissolution of FGD (Fig. 4b and 4c). There was a gradual increase in amorphous secondary phases observed by the increase in lower intensity peaks. More prominent peaks corresponding to the formation of AFt (ettringite CS'H) are observed, confirming the presence of the phases responsible for the sudden decrease in the resistance of specimens with the replacement of 75% of FGD. In addition, the peaks of AFm (monosulfoaluminate CS'A) are superimposed on the Aft (Fig 4d). In conclusion, it can also be noted that the greater the addition of FGD, the more amorphous material is formed, which can be observed in the amount of secondary peaks of lower intensity that gradually became visible.

Fig. 3. Hourglass-shaped specimen

Table 6. Experimental results for fresh state tests

		FGD0	FGD25	FGD50	FGD75
Cement(g)		500	375	250	125
FGD (g)		0	125	250	375
Water (g)		135	215	275	325
Water/cement ratio		0.27	0.43	0.55	0.65
Setting time	Initial (min)	330	-	-	3
	Final (min)	350	-	-	5

Table 7. Mixture proportions of concretes

Sample	Cement (g)	FGD (g)	Fine aggregate (g)	Water (g)
FGD0	624	0	4 x (468)	300
FGD25	468	156	4 x (468)	300
FGD50	312	312	4 x (468)	330
FGD75	156	468	4 x (468)	385

Table 8. Characterization of the tested specimens

Sample	Days	Compressive Strenght (MPa)	Derived Standard Deviation (%)	Slump (mm)	Water/ Cement (%)
FGD0	1	16.36	1.54	169	0.48
	3	27.21	5.07	169	0.48
	7	29.43	5.68	168	0.48
	28	37.12	2.70	168	0.48
	91	41.63	4.00	168	0.48
FGD25	1	6.02	0.00	160	0.48
	3	6.90	5.45	160	0.48
	7	7.86	4.26	160	0,48
	28	10.91	3.45	160	0.48
	91	14.71	2.27	160	0.48
FGD50	1	1.00	0.00	160	0.53
	3	3.51	0.00	160	0.53
	7	4.51	0.00	160	0.53
	28	6.02	0.00	160	0.53
	91	6.90	5.00	160	0.53
FGD75	28	3.01	0.00	160	0.62

Table 9. Crystalline phase contents of the cement specimens at 28 days

Phase	FGD0	FGD25 (%)	FGD50	FGD75
Quartz	22.0	27.0	13.1	8.00
Alite	4.30	1.70	1.51	0.40
Belite	4.60	7.60	8.54	2.00
Celite	0.40	1.44	2.50	0.50
Ferrite	2.20	2.10	5.15	1.00
Portlandite	16.9	4.30	3.16	0.90
Silicate	18.1	19.9	14.6	20.0
Calcium sulfate	12.5	16.0	39.3	60.0
Ettringite	16.0	20.0	12.2	9.00

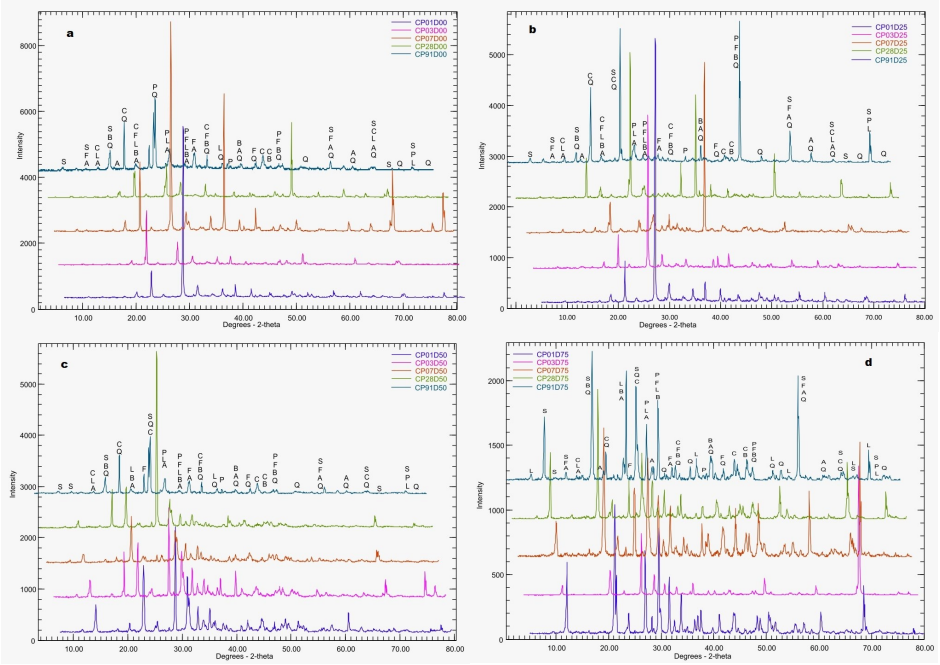

Fig. 4. XRD patterns of cement paste with different FGD content: (a) 0; (b) 25%; (c) 50%; (d) 75% (Q = Quartz (SiO_2); A – Alite (C_3S); B – Belite (C_2S); L – Celite (C_3A); F – Ferrite (C_4AF); P – Portlandite (CH); C – Silicate (CSH); S –Sulfate AFt-Ettringite (CS'H))

The identified phases were quantified using the Rietveld method of X-ray powder diffraction measurements (Fig. 4) for specimens at 28 days and the results are shown Table 9. The decrease in crystallinity of the quartz (Q) phase as a function of the increase in the amount of calcium sulfate (C'SH) caused a decrease in the mechanical strength of the specimens. Furthermore, there was a decrease in the alite phase (C_3S), responsible for the strength of mortars at early ages, and an increase in the belite phase (C_2S).

The belite phase present a lower reaction rate and is responsible for the resistance at older ages, in this case, the amount of belite accumulated was proportional to the addition of FGD, indicating the cause of the decrease in the resistance of the specimens, except by FGD 75, which changed to a hardened state within minutes of molding.

In the diffractograms (Fig. 4) is also possible to observe the reduction of reaction rate of the celite phase (C_3A), responsible for the formation of aluminate and ferroaluminate crystals and in the final strength of the solid state. The decrease in portlandite (CH) phase by the consumption of dissolved sulfate ions contributed to the formation of more calcium sulfate phases.

3.4.3 Leaching and solubilization of the cement specimens

The specimens with 0, 25%, 50% and 75% of FGD as cement substitute were submitted to leaching and solubilization tests for solid waste classification according to Brazilian regulation. The leaching and solubilization tests were carried out in order to determine the potential leachability of selected elements, and the possibility of transferring those elements to the environmental media.

Tables 10 and 11 shows the results of the acetic acid leaching and water solubilization tests carried out with cement specimens, respectively, and the maximum value allowed determined by the Brazilian standard ABNT NBR10004 [41]. No element was present in a quantity greater than the maximum value allowed by the leaching test (Table 10). The results of solubilization indicated that chromium and sulfate concentrations are above the maximum concentration allowed by Brazilian standard ABNT NBR 10004 [41] for all materials (Table 11). The cement specimens can be classified as a Class II-A material (non-hazardous non-inert).

4. CONCLUSION

The present study examined the properties of specimens with 0%, 25%, 50%, and 75% cement replaced by FGD gypsum. FGD gypsum consisted mainly of sulfur and calcium, which had a total weight of about 89%. The pozzolanic activity assay showed that FGD has high reactivity with lime. Although a reduction in compressive strength was observed matrices containing 25% and 50% of FGD gypsum have potential as use in non-structural civil construction materials. In the case of 75% by mass of replacement, the FGD showed the behavior of an accelerating setting additive. The utilization of FDG gypsum for producing cementitious matrices can directly result in a lower usage of natural resource and encourage circular economy, since is a value-added way for waste management. Additionally, can contribute towards the achievement of SDG 12 and FDG gypsum can be employed to minimize the GHG emissions associated with the construction sector.

Table 10. Concentration of elements leachate from cement specimens and allowed limit values

Element	Leachate extract (mg L^{-1})				Allowed Limit (mg L^{-1})
	FGD-0	FGD-25	FGD-50	FGD-75	
Ag	< 0.1	< 0.1	< 0.1	< 0.1	5.0
As	0.13 ± 0.01	0.112 ± 0.007	0.12 ± 0.007	0.12 ±0.01	1.0
Ba	0.2149±0.0008	0.1628±0.0006	0.1097±0.0004	0.066±0.0005	70
Cd	0.1937±0.0009	0.212±0.001	< 0.1	< 0.1	0.5
Cr	< 0.05	< 0.05	0.052 ± 0.008	0.0575 ± 0.003	5.0
Hg	< 0.05	< 0.05	< 0.05	< 0.05	0.1
Pb	0.140 ± 0.009	0.16 ± 0.01	0.188 ±0.005	0.2 ±0.008	1.0
Se	0.076 ± 0.005	0.067±0.002	0.07±0.002	0.07±0.003	1.0

Table 11. Concentration of elements solubilized from cement specimens and allowed limit values

Element\	Solubilized extract (mg L^{-1})				Allowed Limit (mg L^{-1})
	FGD-0	FGD-25	FGD-50	FGD-75	
Ag	< 0.05	< 0.05	< 0.05	< 0.05	0.05
Al	0.1016±0.0005	0.10±0.006	0.101±0.006	0.101±0.008	0.2
As	< 0.05	< 0.05	< 0.05	< 0.05	0.01
Ba	0.1760±0.0008	0.149±0.001	0.116±0.002	0.1193±0.0005	0.7
Cd	< 0.05	< 0.05	< 0.05	< 0.05	0.005
Cr	0.062±0.001	0.0671±0.0004	0.0551±0.0002	0.0604±0.0004	0.05
Cu	< 0.1	< 0.1	< 0.1	< 0.1	2.0
Fe	< 0.05	< 0.05	< 0.05	< 0.05	0.3
Hg	< 0.05	< 0.05	< 0.05	< 0.05	0.001
Mn	< 0.05	< 0.05	< 0.05	< 0.05	0.1
Na	8.8±0.2	7.1±0.1	80±6	67±5	200
Pb	< 0.05	< 0.05	< 0.05	< 0.05	0.01
Se	< 0.05	< 0.05	< 0.05	< 0.05	0.01
Zn	0.0636 ±0.0007	< 0.05	< 0.05	< 0.05	5.0
sulfate	666.8±0.07	818.5±0.1	1137.5±0.3	1241.0±0.1	250

AUTHOR INFROMATION

Corresponding Author
*Email : dfungaro@ipen.br

ORCID
Denise A. Fungaro : 0000-0003-1618-0264
Juliana de C. Izidoro : 0000-0002-3466-5196
R.H.N. Bibiano : 0000-0003-0452-3231

ACKNOWLEDGEMENT

The authors are grateful to IPT (Institute for Technological Research, SP) and Pampa Sul Thermoelectric Power Plant for providing FGD sample.

REFERENCES

[1] Ellis, L. D.; Badel, A. ; Chiang, M. L.; Park, R. J. & Chiang, Y. M. (2020). Toward electrochemical synthesis of cement-An electrolyzer-based process for decarbonating $CaCO_3$ while producing useful gas streams. Proceedings of the National Academy of Sciences of the United States of America, 117, pp.12584-1259.

[2] UNEP (2007). United Nations Environment Programme. Buildings and climate change; ISBN: 978 -92-807-2795-1.

[3] ECTP. European Construction Technology Platform Strategic Research Agenda for the European Construction Sector. Achieving a sustainable and competitive construction sector by 2030; 2005.

[4] Nunes, L. J. R. (2023). The Rising Threat of Atmospheric CO_2: A Review on the Causes, Impacts, and Mitigation Strategies. Environments, 10, pp. 66-88.

[5] Benhelal, E.; Shamsaei, E. & Rashid, M. I. (2021). Challenges against CO_2 abatement strategies in cement industry: A review. Journal of Environmental Sciences, 104, pp. 84-101.

[6] Nasr, M. S.; Shubbar, A. A.; Abed, Z. A. & Ibrahim, M. S. (2020). Properties of eco-friendly cement mortar contained recycled materials from different sources. Journal of Building Engineering, 31, pp.101444.

[7] Bacarji, E. D.; Toledo filho, R.; Koenders, E. A. B.; Figueiredo, E. P. & Lopes, J. L. M. P. (2013). Sustainability perspective of marble and granite residues as concrete Fillers. Construction and Building Materials, 45, pp. 1-10.

[8] Córdoba, P. (2015). Status of Flue Gas Desulphurisation (FGD) systems from coal-fired power plants: Overview of the physic-chemical control processes of wet limestone FGDs. Fuel, 144, pp. 274-286.

[9] Sithole, T.; Mashifana, T.; Mahlangu, D. & Tchadjie, L. (2021). Physical, Chemical and Geotechnical Characterization of Wet Flue Gas Desulfurization Gypsum and Its Potential Application as Building Materials. Buildings, 11, pp.500-520.

[10] Caillahua, M. C. & Moura, F. J. (2018). Technical feasibility for use of FGD gypsum as an additive setting time retarder for Portland cement. Journal of Materials Research and Technology, 7, pp. 190-197.

[11] Jiang, L.; Li, C.; Wang, C.; Xu, N. & Chu, H. (2018). Utilization of Flue Gas Desulfurization Gypsum as an Activation Agent for High-Volume Slag Concrete. Journal of Cleaner Production, 205, pp.589-598.

[12] Chandara, C.; Azizli, K. A. M.; Ahmad, Z. A. & Sakai, E. (2009). Use of waste gypsum to replace natural gypsum as set retarders in portland cement. Waste management, 29, pp 1675–1679.

[13] ABNT NBR 11578. 1991: Cimento Portland composto. Rio de Janeiro (in Portuguese).

[14] ABNT NBR 7214, 2015. Areia normal ensaio cimento – Especificação. Rio de Janeiro (in Portuguese).

[16] ABNT NBR NM 18, 2012. Cimento Portland - Análise química - Determinação de perda ao fogo. Rio de Janeiro (in Portuguese).

[17] ABNT NBR 14656, 2001.Cimento Portland e matérias-primas – Análise química por espectrometria de raios X – Método de ensaio. Rio de Janeiro (in Portuguese).

[18] ABNT NBR NM 13, 2013. Cimento Portland - Análise química - Determinação de óxido de cálcio livre pelo etileno glicol. Rio de Janeiro (in Portuguese).

[19] ABNT NBR NM 15, 2012. Cimento Portland – Análise química - Determinação de resíduo insolúvel. Rio de Janeiro (in Portuguese).

[20] ABNT NBR NM 6473, 2003. Cal virgem e cal hidratada - Análise química. Rio de Janeiro (in Portuguese).

[21] ABNT NBR 11579, 2012. Cimento Portland - Determinação do índice de finura por meio da peneira 75 μm (nº 200). Rio de Janeiro (in Portuguese).

[22] ABNT NBR 16605, 2017. Cimento Portland - Determinação da massa específica. Rio de Janeiro (in Portuguese).

[23] ASTM C1365, 2018. Standard Test Method for Determination of the Proportion of Phases in Portland Cement and Portland-Cement Clinker Using X-Ray Powder Diffraction Analysis (in Portuguese).

[24] ABNT NBR NM 24, 2003. Materiais pozolânicos - Determinação do teor de umidade. Rio de Janeiro (in Portuguese).

[25] ABNT NBR 16607, 2017. Cimento Portland - Determinação dos tempos de pega. Rio de Janeiro (in Portuguese).

[26] ABNT NBR 16372, 2015. Cimento Portland e outros materiais em pó - Determinação da finura pelo método de permeabilidade ao ar (método de Blaine) (in Portuguese).

[27] ABNT NBR 16606, 2018. Cimento Portland - Determinação da pasta de consistência normal. Rio de Janeiro (in Portuguese).

[28] ABNT NBR 5751, 2015. Materiais pozolânicos - Determinação da atividade pozolânica com cal aos sete dias. Rio de Janeiro (in Portuguese).

[29] ABNT NBR 5752, 2014. Materiais pozolânicos - Determinação do índice de desempenho com cimento Portland aos 28 dias. Rio de Janeiro (in Portuguese).
[30] ABNT NBR NM 248, 2003. Agregados, determinação da composição granulométrica. Rio de Janeiro (in Portuguese).
[31] ABNT NBR NM ISO 3310-1, 2010. Peneiras de ensaio - Requisitos técnicos e verificação. Parte 1: Peneiras de ensaio com tela de tecido metálico. Rio de Janeiro (in Portuguese).
[32] ABNT NBR 7211, 2019. Agregados para concreto - Especificação. Rio de Janeiro (in Portuguese).
[33] ABNT NBR NM 52, 2009. Agregado miúdo - Determinação da massa específica e massa específica aparente. Rio de Janeiro (in Portuguese).
[34] ABNT NBR 7215, 1996. Cimento Portland - Determinação da resistência à compressão. Rio de Janeiro (in Portuguese).
[35] ABNT NBR 9479, 2009. Argamassa e Concreto - Câmaras úmidas e tanques para cura de corpos-de-prova. Rio de Janeiro (in Portuguese).
[36] Bibiano, R. H. N. (2021). Feasibility study of adding of sulfated ash generated in a coal-fired power plant in cement industry. Energy and Nuclear Research Institute: Dissertation. (in Portuguese).
[37] ABNT NBR 5739, 2018. Concreto - Ensaio compressão corpos de prova cilíndricos. Rio de Janeiro (in Portuguese).
[38] ABNT NBR7223, 1992. Concreto - Determinação da consistência pelo abatimento do tronco de cone (in Portuguese).
[39] ABNT NBR 10005, 2004. Procedimento para obtenção de extrato lixiviado de resíduos sólido. Rio de Janeiro (in Portuguese).
[40] ABNT NBR 10006, 2004. Procedimento para obtenção de extrato solubilizado de resíduos sólidos. Rio de Janeiro (in Portuguese).
[41] ABNT NBR 10004, 2004. Resíduos sólidos – Classificação. Rio de Janeiro (in Portuguese).
[42] Mansur, A. A. P.; Nascimento, O. L.; Vasconcelos, W. L. & Mansur, H. S. (2008). Chemical Functionalization of Ceramic Tile Surfaces by Silane Coupling Agents: Polymer Modified Mortar Adhesion Mechanism Implications. Materials Research, 11, pp. 293-302.
[43] Nogueira, J R. (2011). Recycling ash: feasibility study for the production of building blocks from the residual fly ash of a fluidized bed reactor. Universidade de São Paulo, São Carlos: Dissertation.
[44] Kurkçu, M. (2006). Utilization on fly ash from fluidized combustion of a turkish lignite in production of blended cements. Middle East Technical University: Ph.D. Thesis.
[45] ABNT NBR 16697, 2018. Cimento Portland - Requisitos. Rio de Janeiro (in Portuguese).
[46] Teixeira, J. M. C. (2013). Use of coal combustion products as additives in the production of mortar for coating material. Universidade Federal do Ceará: Dissertation (in Portuguese).
[47] Witzke, F. B. (2018). Properties of structural concretes containing fly ash in partial replacement of Portland cement. Universidade do Estado de Santa Catarina: Dissertation (in Portuguese).
[48] Santana, R. R. (2002). Characterization and mineralogical reconstruction of coal, kaolin, limestone and sulphated ash generated at the temperature of a fluidized bed aiming at its application in the cement industry. Universidade Federal do Rio Grande do Sul: Ph.D. Thesis (in Portuguese).
[49] Scheinherrová, L.; Doleželová, M.; Havlín, J. & Trník, A. (2018). Thermal analysis of ternary gypsum-based binders stored in different environments. Journal of Thermal Analysis and Calorimetry, 133, pp. 177–188.
[50] Jelenić, I.; Panović, A.; Halle, R. & Gaćeša, T. (1977). Effect of gypsum on the hydration and strength development of commercial portland cements containing alkali sulfates. Cement and Concrete Research, 7, pp. 239–245.
[51] Castro, R. P. V. (2016). Characterization of solids and development of analytical methodology for monitoring the oxidative treatment of solid waste from desulphurization of exhausted phases of a coal-fired power plant. Universidade Federal do Rio de Janeiro: Dissertation (in Portuguese).
[52] Siddique, R. (2010). Utilization of coal combustion by -products in sustainable construction materials. Resources, Conservation and Recycling. 54, pp.1060-1066.
[53] Qiao, X. C.; Poon, C. S. & Cheeseman, C. (2006). Use of flue gas desulphurisation (FGD) waste and rejected fly ash in waste stabilization/solidification systems. Waste Management, 26, pp.141-149.
[54] Marinković. S.; Kostić-pulek, A.; Logar, V. & Trifunović, P. (2005). Recycling of waste fgd gypsum. 32nd International Conference of SSCHE. Tatransk´e Matliare, Slovakia, May 23–27.
[55] Li, Y., Zhang, F.; Wang, S.; Luo, C.; Zhao, B.; Zhuo, Y. & Chen, C. (2010). Environmental impact on alkali soil amelioration using FGD gypsum. Journal of Agricultural Science and Technology, 12, pp. 86-89.